

## Photocatalysis

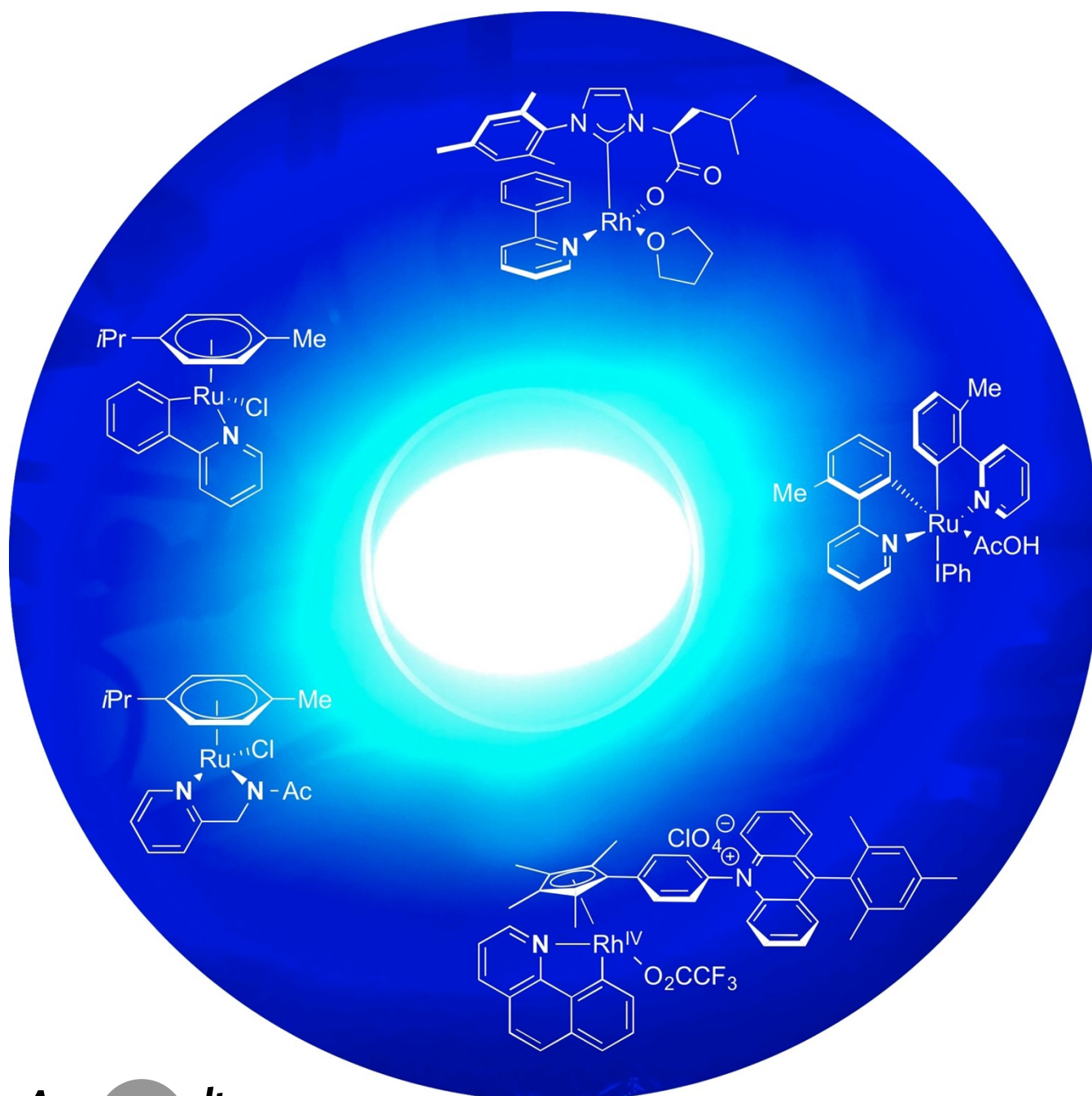
How to cite: *Angew. Chem. Int. Ed.* **2022**, *61*, e202201743

International Edition: doi.org/10.1002/anie.202201743

German Edition: doi.org/10.1002/ange.202201743

# Visible-Light-Induced, Single-Metal-Catalyzed, Directed C–H Functionalization: Metal-Substrate-Bound Complexes as Light-Harvesting Agents

Chao Pei, Claire Empel, and Rene M. Koenigs\*



**Abstract:** C–H functionalization represents one of the most rapidly advancing areas in organic synthesis and is regarded as one of the key concepts to minimize the ecological and economic footprint of organic synthesis. The ubiquity and low reactivity of C–H bonds in organic molecules, however, poses several challenges, and often necessitates harsh reaction conditions to achieve this goal, although it is highly desirable to achieve C–H functionalization reactions under mild conditions. Recently, several reports uncovered a conceptually new approach towards C–H functionalization, where a single transition-metal complex can be used as both the photosensitizer and catalyst to promote C–H bond functionalization in the absence of an exogenous photosensitizer. In this Minireview, we will provide an overview on recent achievements in C–H functionalization reactions, with an emphasis on the photochemical modulation of the reaction mechanism using such catalysts.

## 1. Introduction

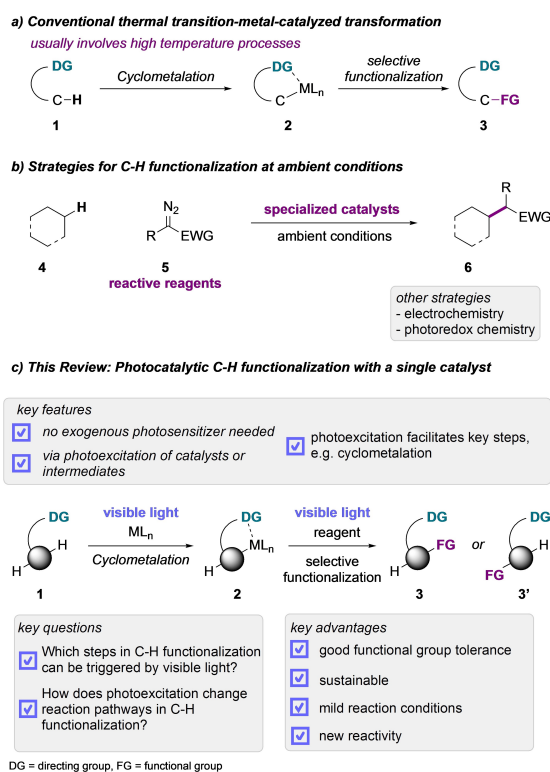
The selective functionalization of C–H bonds is an important strategy to increase molecular complexity and to introduce new functional groups onto molecular scaffolds—ideally from starting materials that do not require elaborate prefunctionalization.<sup>[1–12]</sup> As such, C–H functionalization reactions have been recognized as one of the key approaches to reduce the environmental and economic impact of chemical synthesis and has found applications in material sciences,<sup>[13,14]</sup> biological chemistry, and drug discovery.<sup>[15–18]</sup> The assistance of directing groups has been identified as a central strategy to direct a transition-metal catalyst into the proximity of a specific C–H bond in a molecule to facilitate selective cyclometalation and subsequent functionalization.<sup>[10–12,19–22]</sup> One of the key challenges in the functionalization of C–H bonds lies, however, in the intrinsic low reactivity of C–H bonds, which often require forcing reaction conditions, such as highly elevated reaction temperatures, which in turn may lead to reduced selectivity, reduced functional group tolerance, or limited applicability (Scheme 1a). There is, however, a high demand to achieve C–H functionalization reactions with high regio- and chemoselectivity under mild reaction conditions—ideally at room temperature. The development of strategies to achieve this goal can be regarded as one of the key drivers to leverage such reactions to the challenges of the 21st century and to further reduce the environmental and economic impact of chemical synthesis.<sup>[23]</sup>

In this context, recent developments have led to several main approaches that are currently in the focus of synthetic chemists to achieve this goal. One strategy envisages the development of state-of-the-art catalysts and reactive reagents that can be used under ambient conditions (Scheme 1b).<sup>[2,3,5,24–29]</sup> Further alternatives lie in the use of catalysts based on earth-abundant metals<sup>[30–32]</sup> or the use of electrochemical or photocatalytic methods that rely on the

redox chemistry of substrates and/or catalysts.<sup>[22,33–37]</sup> These strategies are not in the focus of this Minireview and the reader is referred to recent review articles on these topics.

A conceptually distinct, recent approach builds on the photochemical properties of metal complexes, which are often intensely colored, absorb visible light, and can be used as both the photosensitizer and catalyst without the need for an exogenous photosensitizer.<sup>[30,31,38–40]</sup> In the context of C–H functionalization reactions, this approach involves a single transition-metal catalyst that is capable of both converting photonic energy into usable chemical energy and enabling key elementary steps to allow the C–H functionalization of organic molecules.

The large diversity of metal complexes used for—or occurring as intermediates in—C–H functionalization offers a vast potential to facilitate different elementary steps in C–H functionalization reactions (Scheme 1c). Photochemi-



**Scheme 1.** C–H functionalization strategies and opportunities for light-mediated C–H functionalization via cyclometalated intermediates.

[\*] C. Pei, C. Empel, Prof. Dr. R. M. Koenigs  
RWTH Aachen University, Institute of Organic Chemistry  
Landoltweg 1, 52074 Aachen (Germany)  
E-mail: rene.koenigs@rwth-aachen.de

© 2022 The Authors. Angewandte Chemie International Edition published by Wiley-VCH GmbH. This is an open access article under the terms of the Creative Commons Attribution Non-Commercial License, which permits use, distribution and reproduction in any medium, provided the original work is properly cited and is not used for commercial purposes.

cal excitation allows the manipulation of a plethora of divergent reaction pathways that can involve, for example, ligand exchange, C–H metalation, electron or proton transfer, catalyst release through reductive elimination, and many others. Thus, the photoexcitation of a colored metal complex or reaction intermediate can facilitate a range of different key mechanistic events in C–H functionalization reactions and will be discussed in this Minireview in the order of the general, elementary steps of the C–H functionalization reactions:

- light-mediated C–H metalation
- light-mediated C–C coupling
- light-mediated ligand deprotonation
- light-mediated reductive elimination

## 2. Light-Mediated C–H Metalation

C–H metalation constitutes one of the fundamental reaction steps in directing-group-assisted C–H functionalization, which was recently uncovered to be accessible under photochemical conditions at room temperature. In this context, Baslé and co-workers reported in 2019 on the application of the bidentate carboxylate NHC ligand based Rh<sup>I</sup> catalyst **8**, that absorbs light in the blue light region for the photochemical aromatic and aliphatic C–H borylation of 2-aryl(4-methylpyridine) featuring a photochemical cyclometalation step.<sup>[41]</sup> Simple 2-phenylpyridine gave the desired *ortho*-borylation product only in 50% yield with modest regioselectivity, which might be caused by competitive borylation on the pyridine moiety.<sup>[42]</sup> Under optimized conditions, the authors examined various arylated pyridine- and isoquinoline-based substrates, which proved compatible and afforded

the C(sp<sup>2</sup>)–H or C(sp<sup>3</sup>)–H borylation products—or more precisely the corresponding hydroxylated product after oxidative workup—in good yield under mild photochemical reaction conditions (Scheme 2).

In a series of control experiments, Baslé and co-workers provided mechanistic insight into the reaction. First, different radical inhibitors, including butylated hydroxytoluene (BHT) and TEMPO, suppressed the reaction slightly, which excludes the participation of a radical process. Furthermore, a KIE value of 2.1 suggests that the C–H bond-breaking process should be the rate-determining step. With regards to the catalyst, stoichiometric experiments revealed the formation of a cyclometalated Rh–H complex under photochemical conditions, with no reaction occurring in the dark. On the basis of these observations, the authors postulated that the photosensitive NHC–Rh<sup>I</sup> catalyst undergoes a metal-to-ligand charge transfer (MLCT) during photochemical excitation, which then promotes oxidative addition into the *ortho*-C–H bond. Further reaction with B<sub>2</sub>pin<sub>2</sub> leads to the corresponding Rh<sup>III</sup>-boryl complex with HBpin as a by-product, followed by reductive elimination to give the desired *ortho*-borylated product. However, the mechanism of the borylation step remains speculative.

The role of the photochemical excitation of the catalyst in this borylation reaction thus lies within promoting the C–H bond-activation step at room temperature and opening up reaction pathways that are inaccessible in the dark or under more forcing conditions (Scheme 2).

It is worth mentioning that shortly after this work, the Tanaka group reported a detailed study on such photochemical C–H borylation reactions using Rh<sup>III</sup> catalysts with and without external photosensitizers. This reaction, however, only proceeds in only moderate yield for a single



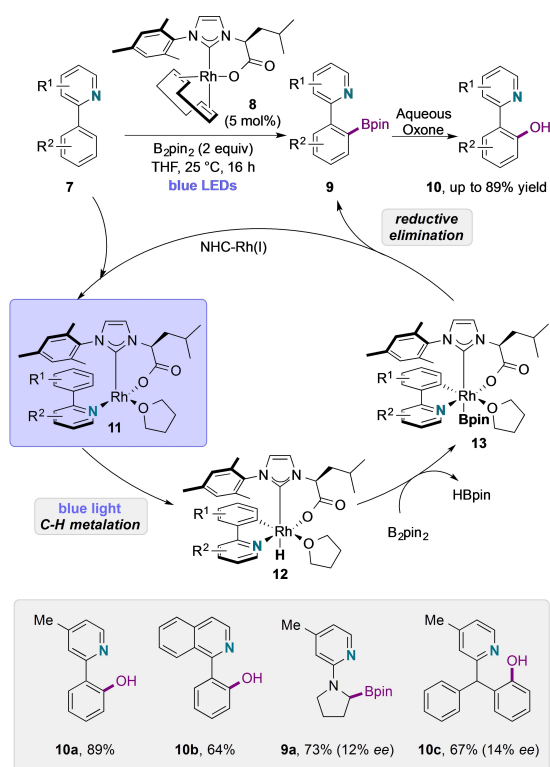
Chao Pei received his B.Sc. from Soochow University in 2016. He then completed his M.Sc. under the supervision of Prof. Xinfang Xu at the same university in 2019. Currently, he is pursuing his Ph.D. under the supervision of Prof. Rene M. Koenigs at RWTH Aachen University. His research interests focus on theoretical calculations and mechanistic studies of photochemistry and metal catalysis.



Rene M. Koenigs obtained his Ph.D. from RWTH Aachen University under the supervision of Prof. Magnus Rueping. After an industrial stay with Grünenthal GmbH working on GPCR and ion channel targets, he was appointed as junior professor at RWTH Aachen University. His research interests focus on reactive intermediates, photochemistry and photocatalysis, continuous-flow chemistry, and fluorine chemistry.



Claire Empel studied chemistry at RWTH Aachen University and the University of New South Wales. Currently, she is a Ph.D. student in the group of Prof. Rene M. Koenigs, funded by a Kekulé Scholarship from the Fonds der Chemischen Industrie. Her research is focused on experimental and theoretical studies on photochemical and metal-catalyzed carbene and nitrene transfer reactions.



**Scheme 2.** Photoinduced rhodium-catalyzed *ortho*-C–H borylation reactions.

example in the absence of an external photosensitizer, and an external iridium-based photocatalyst is needed to obtain high yields. This reaction proceeds via the in situ formation of a  $\text{Rh}^{\text{I}}$  complex that undergoes cyclometalation. The

cyclometalated complex can then undergo photoexcitation to access a triplet intermediate, which engages in single electron transfer reactions.<sup>[43]</sup>

### 3. Light-Mediated C–C Coupling

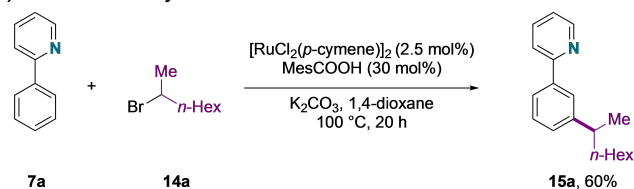
In this section we discuss approaches in which a substrate engages in the formation of a cyclometalated complex. Photoexcitation of this complex is then key to access single electron transfer reactions to enable the C–C coupling of radical intermediates and the cyclometalated complex. These reactions thus resemble classic thermal C–H functionalization reactions; however, photochemistry is key to unlocking the C–C coupling event.

#### 3.1. Photoinduced C–H Alkylation Reactions

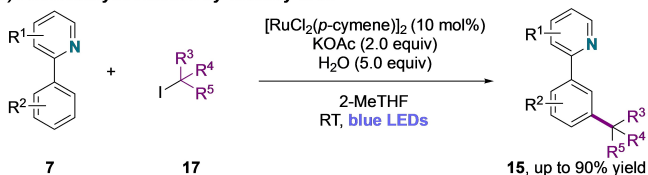
Another strategy involves the generation of radical intermediates by single electron transfer reactions from the photoexcited state of key intermediates in C–H functionalization reactions, which then leads to the formation of new C–C bonds through a radical mechanism. In 2019, the Ackermann and Greaney groups independently identified a novel photochemical strategy that allows the ruthenium-catalyzed *meta*-C–H alkylation reaction of 2-aryl pyridines.<sup>[44,45]</sup>

Such aromatic *meta*-C–H functionalizations constitute a key challenge in organic synthesis and was initially reported in 2013 by Hofmann and Ackermann using a  $\text{Ru}^{\text{II}}$  catalyst, 2-aryl pyridines as substrates, and secondary alkyl halides as reaction partners under thermal conditions (Scheme 3a).<sup>[46]</sup> However, such *meta*-C–H functionalization reactions usually

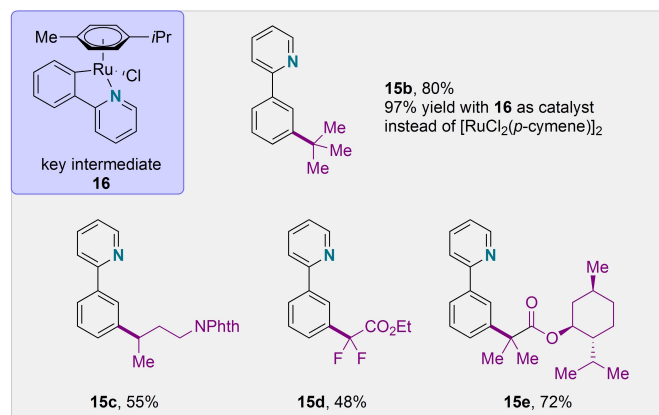
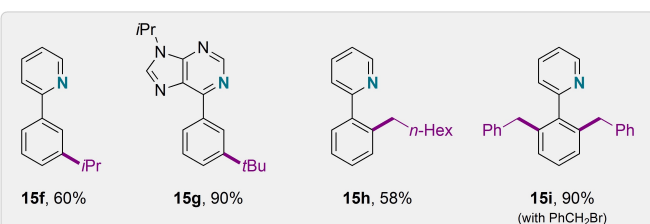
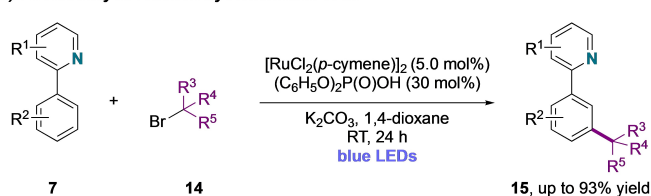
#### a) Thermal reaction by Ackermann et al.



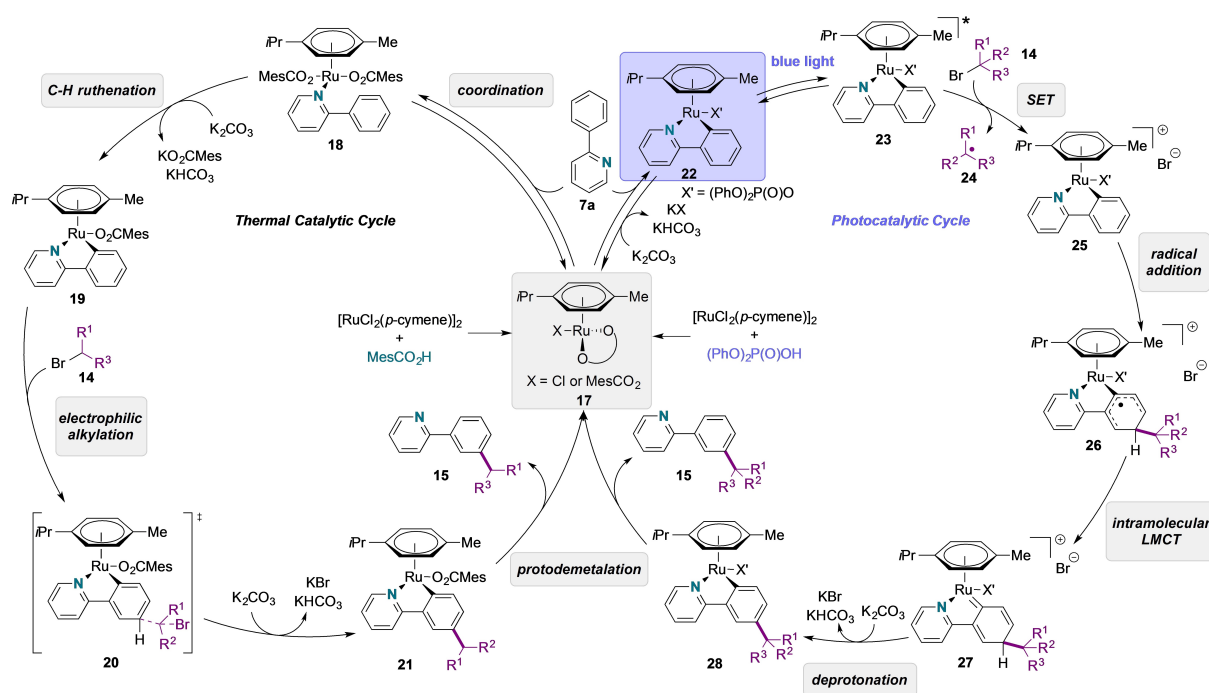
#### c) Photocatalytic reaction by Greaney et al.



#### b) Photocatalytic reaction by Ackermann et al.



**Scheme 3.** a) Thermal alkylation reactions. b, c) Photoinduced ruthenium-catalyzed *meta*-C–H alkylation reactions with alkyl halides.



**Scheme 4.** Comparison of the proposed mechanisms for thermal and photocatalytic *meta*-C–H alkylation reactions.

require high reaction temperatures, which affects the functional group tolerance and thus necessitates the development of new synthetic methods with high selectivity under mild reaction conditions.

In the recent reports by the Ackermann and Greaney groups, the authors showed that such C–H functionalization reactions can be performed under photochemical conditions at room temperature (Scheme 3b,c). Similar to the conventional thermal C–H functionalization reaction, both groups showed that  $[\text{RuCl}_2(p\text{-cymene})]_2$  initially forms an intermediate ruthenacycle with 2-aryl pyridines. This cyclometalated ruthenium complex absorbs in the visible-light region and can undergo a photochemical C–H functionalization reaction, as shown in control experiments with the isolated ruthenacycle. A key difference to the previous report on thermal *meta*-C–H functionalization lies within the reaction scope: whereas only simple alkyl halides were reported in the initial thermal study, the authors showed that a broad range of different functional groups is tolerated under the photochemical conditions. Specifically, a variety of tertiary and secondary unactivated alkyl bromides and synthetically meaningful  $\alpha$ -bromo esters, including naturally occurring compounds, were studied and found to be compatible and provide the desired *meta*-C–H functionalized products in good yields under mild conditions, and thus significantly expands the substrate scope of such *meta*-C–H functionalization reactions. An important difference lies within the additive: carboxylic acids proved ideal under thermal conditions and only low yields were observed with carboxylic acids under photochemical conditions. A pivotal role is thus associated with diphenyl phosphate, which needs to be used as an additive to achieve high efficiency. A rationale as to why the Ru catalyst is more active in the presence of

phosphoric acid under photochemical conditions remains elusive.

To gain insight into the photocatalytic *meta*-selective C–H alkylation reaction, the Ackermann and Greaney groups reported control experiments with both the cyclometalated ruthenium complex **16** as well as  $[\text{RuCl}_2(p\text{-cymene})]_2$ . These experiments included on/off experiments, cyclic voltammetry, fluorescence quenching, and trapping experiments, which provide evidence of the viability of single electron transfer reactions from the photoexcited state of cyclometalated complex **16** and lead to the formation of alkyl radical intermediates as one of the key reactive species. In brief, the reaction only proceeds in the presence of light, but the quantum yield of this transformation is low at 1.6%. Typical radical scavengers prevent or significantly suppress the reaction. The isolated cyclometalated ruthenium complex **16** possesses a weak absorption band in the relevant blue region and an oxidation potential of 0.98 V in DCE (vs. Ag/AgCl).

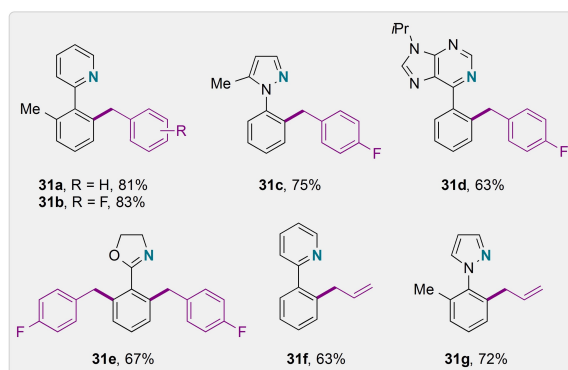
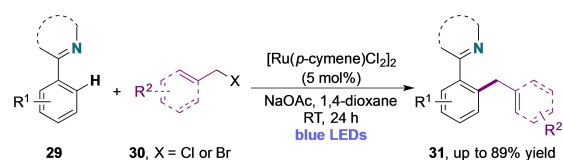
Based on the mechanistic findings, Scheme 4 shows the proposed catalytic cycle, with the thermal catalytic cycle also depicted. An initial reversible C–H ruthenation of 2-phenylpyridine generates the cyclometalated ruthenium complex, which can be assisted by the acid additive. In the thermal cycle, this cyclometalation activates the aromatic ring through the strong directing group effect of the Ru–C( $\text{sp}^2$ )  $\sigma$ -bond, which leads to an  $\text{S}_{\text{E}}\text{Ar}$ -type alkylation by secondary alkyl halides at the *para*-position of the Ru–C( $\text{sp}^2$ ) bond. Under photochemical conditions, such cyclometalated complexes can serve as single-electron donors upon photoexcitation to achieve a single electron transfer process to the alkyl halide, which gives the oxidized, cyclometalated  $\text{Ru}^{\text{III}}$  complex **25**. In the next step, the generated alkyl radical

adds to the *para*-position relative to the Ru–C bond of the aromatic ring. Subsequent intramolecular LMCT and re-aromatization under basic conditions provides the cyclometalated ruthenium complex **28**. Final protodemetalation releases the *meta*-C–H alkylation product and regenerates the ruthenium catalyst **17**.

A comparison of the thermal and photochemical *meta*-C–H functionalizations thus shows a key mechanistic difference: Whereas the cyclometalated ruthenium complex **19** reacts as a nucleophile under thermal conditions, its oxidized form **25** reacts as a radical acceptor under photochemical conditions.

A distinct observation was made by Sagadevan and Greaney when using primary alkyl halides. In this case, a switch in selectivity was observed, with selective *ortho*-C–H functionalization occurring under photochemical conditions (Scheme 5).<sup>[45]</sup> This *ortho*-selectivity is consistent with previous reports on *ortho*-alkylation, which can be reasoned by the low steric demand of primary alkyl halides.<sup>[47]</sup> Highly activated benzyl bromide smoothly reacts to afford the double *ortho*-benzylated product of 2-phenylpyridine in 90% yield under photochemical reaction conditions—the corresponding thermal reaction has not been reported to date. This *ortho*-C–H functionalization was recently studied in more detail by the Ackermann group using benzyl chlorides and allyl bromides.<sup>[48]</sup> Two key strategies were pursued to achieve monoalkylation reactions: a) by blocking the second site for C–H functionalization with a methyl group or b) by the introduction of steric repulsion through the use of a modified directing group. The versatility of this photochemical C–H alkylation was further demonstrated using water as a green reaction medium.

These findings show the unique potential of using a single photosensitive ruthenium catalyst, which has been demonstrated in site-selective C–H alkylation reactions. This methodology avoids the disadvantages of conventional, thermal C–H functionalization reactions.



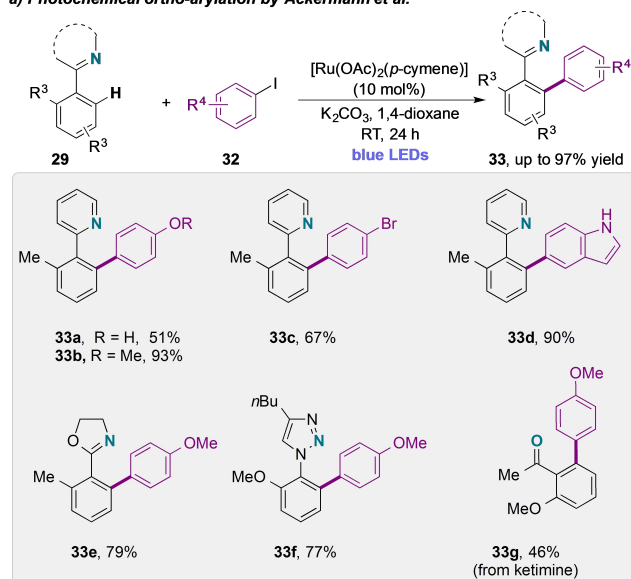
**Scheme 5.** Photoinduced ruthenium-catalyzed *ortho*-C–H alkylation reactions with benzyl or allyl halides.

### 3.2. Photoinduced *ortho*-C–H Arylation Reactions

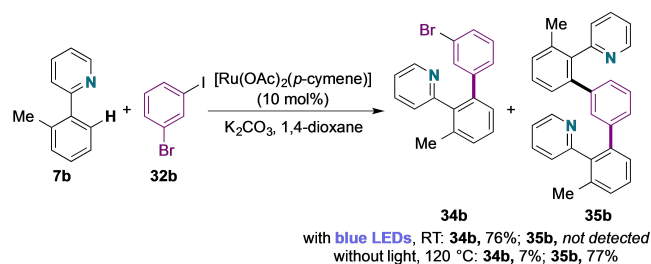
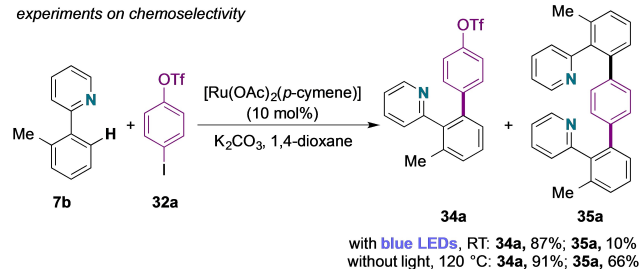
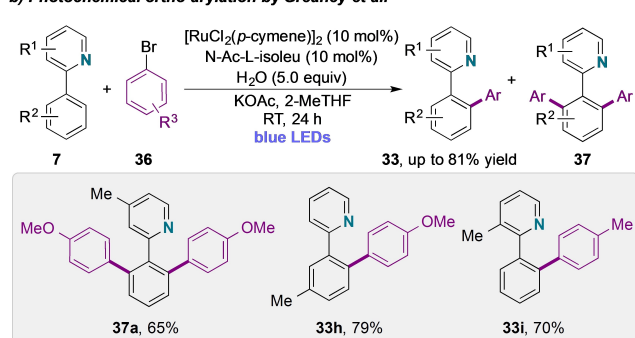
The same research groups expanded this methodology towards *ortho*-C–H arylation reactions with aryl halides.<sup>[49,50]</sup> Such ruthenium-catalyzed *ortho*-C–H arylation was previously explored under thermal conditions involving a ruthenium(II/IV) catalytic cycle with oxidative addition and reductive elimination. However, applications are restricted to high reaction temperatures of typically 100–140 °C.<sup>[51–53]</sup> Under simple irradiation with visible light, the reaction temperature can be significantly lowered to room temperature and highly efficient C–H arylation reactions can be achieved. Both research groups identified carboxylates, such as KOAc, as key additives to enable the *ortho*-C–H arylation. A specific challenge with *ortho*-C–H arylation reactions lies in achieving selective mono- vs. diarylation, and the intrinsically higher susceptibility of the monoarylated product towards cyclometalation<sup>[49]</sup> hampers the development of a chemoselective transformation. Therefore, diarylation reactions can be accessed, whereas monoarylation only occurs if one *ortho*-C–H bond is blocked by a substituent (Scheme 6).

It is noteworthy that the photochemical method provides a greater functional group tolerance compared to traditional thermal conditions. In particular, sensitive functional groups in the aryl iodide reaction partner, including hydroxy, chloro, bromo, carbonyl, indole, and carbazole, are tolerated under the mild reaction conditions and offer key synthetic advantages. In addition, besides 2-aryl pyridines, the Greaney group showed the directing groups could be extended to quinoline and pyrazole heterocycles, whereas the Ackermann group demonstrated the applicability of triazoles, pyrimidines, imidates, pyrazoles, and ketimines as compatible directing groups. Moreover, this photocatalytic strategy shows excellent chemoselectivity in the arylation reaction coupling partners bearing two different halogens or pseudo-halogens. Ackermann and co-workers showed that 4-iodophenyl triflate and 1-iodo-3-bromobenzene undergo selective coupling at the C–I bond, while the bromide or triflate remain untouched. Under thermal conditions, the lack of discrimination of the complementary aryl halides leads to highly selective diarylated products (Scheme 6).<sup>[53]</sup>

From a mechanistic perspective, this C–H arylation proceeds through a distinct pathway, as previously discussed for the *meta*-C–H functionalization reaction.<sup>[46]</sup> A plausible catalytic cycle is initiated by C–H ruthenation to generate a mono-cyclometalated ruthenacycle. This ruthenacycle is assumed to undergo a further ligand exchange through photochemical dissociation of the *p*-cymene ligand and assistance of the carboxylate additive to afford the bis-cyclometalated ruthenacycle **38** (Scheme 7). A control experiment by the Ackermann group with a cyclometalated complex without a cymene ligand as catalyst shows that this *ortho*-C–H arylation can indeed proceed through the base-assisted formation of such bis-cyclometalated complexes and that the cymene ligand is not required in this reaction. The Greaney group performed a set of control experiments that provide evidence for the participation of radical intermedi-

a) Photochemical *ortho*-arylation by Ackermann et al.

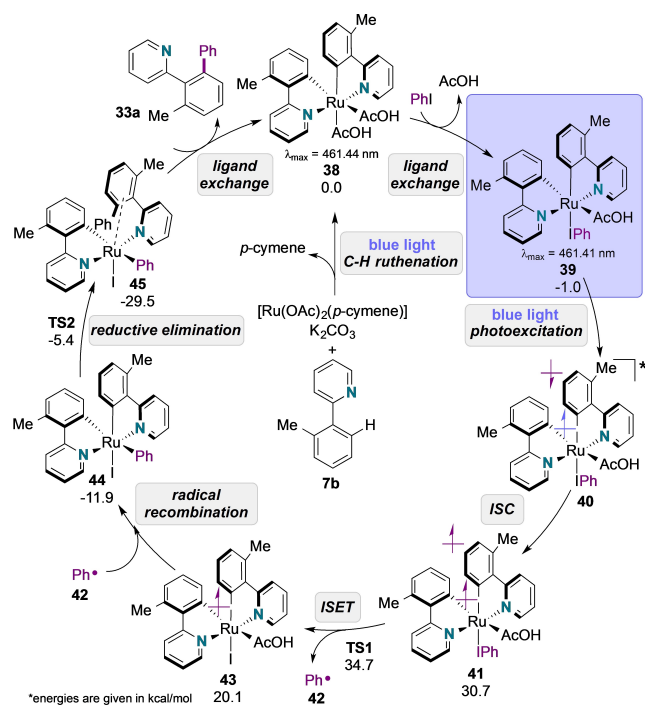
## experiments on chemoselectivity

b) Photochemical *ortho*-arylation by Greaney et al.

**Scheme 6.** Photoinduced ruthenium-catalyzed *ortho*-arylation reactions with aryl halides. a) by Ackermann et al. and b) by Greaney et al.

ates and the photoinduced cleavage of the cymene ligand under the reaction conditions.

Further mechanistic investigations were carried out by (TD)-DFT calculations. These studies reveal that bis-cyclo-



**Scheme 7.** (TD)-DFT calculated mechanism for the ruthenium-catalyzed *ortho*-C–H arylation.

metalated complex 39 possesses an absorption maximum at  $\lambda_{\text{max}} = 461 \text{ nm}$ , which suggests that complex 39 may serve as the photoactive species in the catalytic cycle. Under irradiation with blue light, the singlet excited state of iodoarene-coordinated ruthenacycle complex 40 undergoes intersystem crossing (ISC) to give a long-lived, more-stable triplet species 41 with an activation energy of  $30.7 \text{ kcal mol}^{-1}$ . An outer-sphere electron transfer (OSET) between triplet species 41 and iodobenzene to account for the product formation can be excluded because of the high energy barrier of  $31.8 \text{ kcal mol}^{-1}$  according to Marcus theory and Savéant's model. Instead, a facile inner-sphere electron transfer (ISET) from triplet state complex 41 via the low transition state TS1 with a free energy of  $4.0 \text{ kcal mol}^{-1}$  generates a highly reactive phenyl radical 42 and ruthenium(III) complex 43. Recombination of 42 and 43 gives a stable ruthenium(IV) intermediate 44 to complete the formal oxidative addition step, which is facilitated by visible light. Finally, reductive elimination delivers the *ortho*-arylated product and regenerates the ruthenium catalyst (Scheme 7).

Thus, in this *ortho*-C–H arylation, the role of light is twofold: a) it facilitates the release of the cymene ligand to allow the formation of the bis-cyclometalated ruthenium complex 38 and b) it facilitates the generation a triplet excited state to enable a single-electron transfer and radical generation.

#### 4. Light-Mediated Ligand Deprotonation

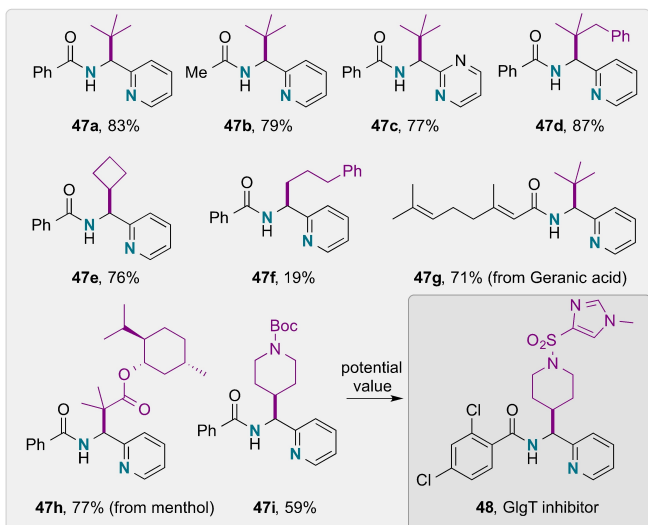
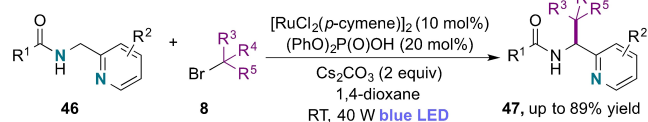
In addition to photoinduced metal-catalyzed site-selective C(sp<sup>2</sup>)-H functionalization, the Koenigs group has recently studied the application of this photochemical strategy towards C(sp<sup>3</sup>)-H functionalization in Ru<sup>II</sup>-catalyzed C(sp<sup>3</sup>)-C(sp<sup>3</sup>) coupling reactions.<sup>[54]</sup> Importantly, control reactions under thermal conditions revealed that this transformation only occurs under photochemical conditions, which thus shows that novel and exclusive reaction modes in C-H functionalization can be accessed under photochemical conditions (Scheme 8).

In this study, the authors showed that, in the presence of [Ru(cymene)Cl<sub>2</sub>]<sub>2</sub> as a catalyst, a chemoselective C(sp<sup>3</sup>)-H functionalization occurred in the benzylic position of methylpyridyl-substituted amides **46** when using alkyl bromide **8** under photochemical conditions. Various tertiary and secondary alkyl bromides were found to be compatible and provide the corresponding benzylic C(sp<sup>3</sup>)-H alkylation products in high yield. Such functionalized pyridine compounds find important applications in medicinal chemistry and organic synthesis.

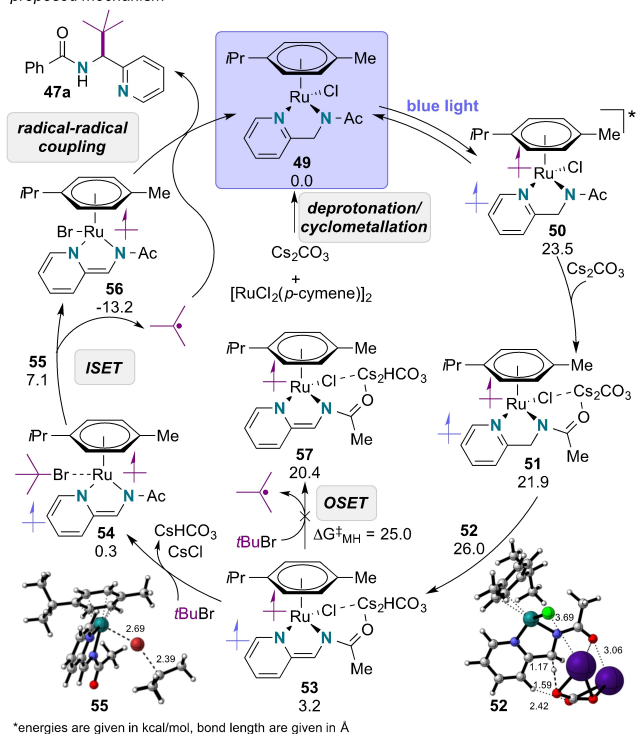
For mechanistic insight, the authors conducted a series of control experiments and combined these with theoretical calculations. Radical trapping reactions with TEMPO and 1,1-diphenylethylene suggest that radical formation is involved in this reaction, which is consistent with the reported aromatic alkylation reactions described in Section 3. Moreover, an on/off experiment indicates that the reaction proceeds only under constant irradiation with light, which suggests that a radical chain process may not be involved. The isolation of the cyclometalated ruthenium complex **49** was highly relevant for a mechanistic proposal. Complex **49** possesses a strong absorption band in the blue light region and was identified as a suitable catalyst for this transformation. Deuterium labeling experiments with D<sub>2</sub>O under basic conditions suggest that irradiation with blue light would facilitate deprotonation of the benzylic C(sp<sup>3</sup>)-H bond of ruthenacycle **51**, which is regarded as the key step in this coupling reaction. As in the initial reports by the groups of Ackermann and Greaney, diphenyl phosphate was found to be a key additive to achieve high reaction efficiency. The role of this acid, however, remains unclear.

To further support the reaction mechanism, detailed computational studies were performed, with a focus on the cyclometalated Ru<sup>II</sup> complex **49** as the catalytically active species. In brief, these studies corroborate the experimental studies and show that the photoexcitation of **49** leads to **50**, which undergoes intersystem crossing to give a triplet complex **51** that can easily undergo a deprotonation reaction under basic conditions with an energy barrier of 4.1 kcal mol<sup>-1</sup>. A subsequent exothermic ligand exchange with alkyl bromides followed by an intramolecular SET process gives an alkyl radical intermediate that finally undergoes radical-radical coupling (Scheme 8).

This work thus showcases that the photochemical excitation of cyclometalated complexes can be used for the deprotonation of C(sp<sup>3</sup>)-H bonds and thereby access novel C-H functionalization pathways.



proposed mechanism



**Scheme 8.** Photoinduced ruthenium-catalyzed C(sp<sup>3</sup>)-C(sp<sup>3</sup>) coupling reaction.

#### 5. Light-Mediated Reductive Elimination

The above-discussed applications build on the use of metal complexes that act as catalysts for the C-H functionalization reaction and as photosensitizers. One of the key drawbacks of this approach lies in the low quantum yields and, thus, the poor photochemical efficiency of these processes, as re-



ported by the Ackermann group.<sup>[44,50]</sup> The introduction of a photosensitizer within the catalyst itself is, therefore, a straightforward approach to cooperatively overcome such limitations, as demonstrated, for example, in the development of hydrogen production photocatalysts.<sup>[55]</sup> Such a system benefits from the simple photoexcitation of a redox-active photosensitizer that can ease intramolecular redox events, thereby accessing unconventional oxidation states of transition-metal catalysts cooperatively.

In this context, the Chang group developed a bimodular rhodium photocatalyst consisting of a Rh<sup>III</sup> metal complex for C–H activation and a light-harvesting group to allow efficient access to photoexcited states (Scheme 9).<sup>[56]</sup> Based on previous studies that indicated a facilitated reductive elimination step from high oxidation states in the presence of external oxidants,<sup>[57]</sup> Chang and co-workers envisioned a modified rhodium catalyst linked to a photosensitizer with a strong absorbance in the visible-light region. In this fundamental study, Chang and co-workers accomplished initial proof-of-concept applications with the C–H functionalization of benzo[*h*]quinolone—more importantly, the authors performed a detailed analysis of the fundamental processes to validate this concept. Frontier molecular orbital analysis showed that excitation of complex **63** results in a

charge transfer between the rhodacycle and the light-harvesting moiety which leads to an internal oxidation to form a transient high-valent Rh<sup>IV</sup> species. Computational studies further substantiate the authors' initial hypothesis of facile reductive elimination from Rh<sup>IV</sup> species (6.0 kcal mol<sup>-1</sup> compared to that of 27.0 kcal mol<sup>-1</sup> in the Rh<sup>III</sup>/Rh<sup>I</sup> process; Scheme 9).

This novel catalyst design thus represents a fundamental example that opens up promising strategies in catalyst design beyond C–H functionalization chemistry to facilitate catalytic processes based on high oxidation-state intermediates with suitable, bimodular catalysts without the need for harsh reaction conditions.

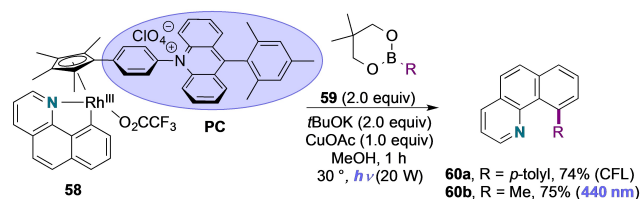
## 6. Summary

Over the past few years, several key conceptual breakthroughs in photochemical C–H functionalization under ambient conditions have been achieved. In this Minireview, we have discussed the use of a single catalyst for both photosensitization and C–H functionalization without the need for external photosensitizers. Depending on the reaction conditions, essentially all the key reaction steps of C–H functionalization reactions—ranging from C–H bond activation or cyclometalation, single-electron transfer and radical formation, ligand-exchange reactions, and ligand backbone deprotonation—can now be facilitated by photochemical excitation of archetypal C–H functionalization catalysts to accelerate reductive elimination. Detailed mechanistic studies have revealed the role of visible light in promoting these transformations. Therefore, this photochemical strategy still holds vast potential to further explore C–H functionalization reactions under mild reaction conditions to provide new synthesis methods. More specifically, this concept now allows the development of C–H functionalizations that are challenging to control under thermal conditions, expand the scope of compatible functional groups, and may serve as an entry for the discovery of novel chemical transformations. For the last case, a limited number of initial reports that describe novel reactivity patterns in C–H functionalization reactions under photochemical conditions already foreshadow potential future advances. Furthermore, the exceptionally mild reaction conditions may prove beneficial to control enantioselective C–H functionalization reactions, which are intrinsically difficult to achieve under thermal conditions. Overall, the advances discussed in this Minireview may serve as a blueprint to provide many new opportunities for further explorations and discoveries.

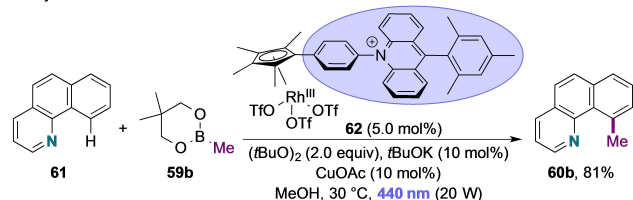
## Acknowledgements

R.M.K. thanks the German Science Foundation and the Fonds of the Chemical Industry for financial support. C.P. gratefully acknowledges the China Scholarship Council for generous support. C.E. gratefully acknowledges the Fonds

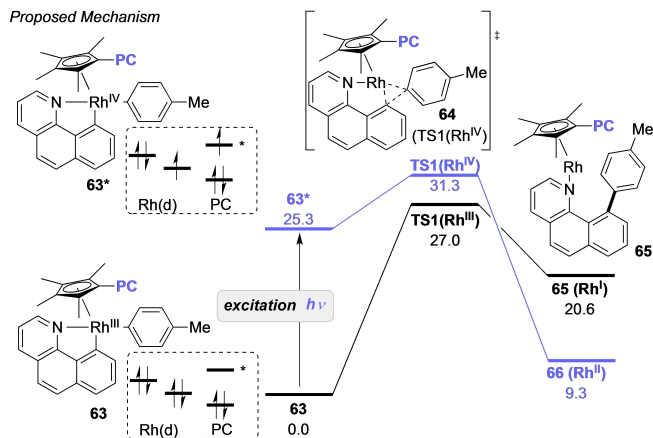
### Stoichiometric C-H functionalization



### Catalytic C-H functionalization



### Proposed Mechanism



**Scheme 9.** Photoinduced C–H alkylation or arylation reactions with a bimodular rhodium catalyst.

of the Chemical Industry for a Kékulé Scholarship. Open Access funding enabled and organized by Projekt DEAL.

### Conflict of Interest

The authors declare no conflict of interest.

**Keywords:** C–H Functionalization · Computational Chemistry · Photocatalysis · Rhodium · Ruthenium

- [1] T. W. Lyons, M. S. Sanford, *Chem. Rev.* **2010**, *110*, 1147–1169.
- [2] M. P. Doyle, R. Duffy, M. Ratnikov, L. Zhou, *Chem. Rev.* **2010**, *110*, 704–724.
- [3] H. M. L. Davies, D. Morton, *Chem. Soc. Rev.* **2011**, *40*, 1857.
- [4] K. R. Campos, *Chem. Soc. Rev.* **2007**, *36*, 1069–1084.
- [5] C. Empel, R. M. Koenigs, *Synlett* **2019**, *30*, 1929–1934.
- [6] C.-S. Wang, P. H. Dixneuf, J.-F. Soulé, *Chem. Rev.* **2018**, *118*, 7532–7585.
- [7] I. A. I. Mkhalid, J. H. Barnard, T. B. Marder, J. M. Murphy, J. F. Hartwig, *Chem. Rev.* **2010**, *110*, 890–931.
- [8] R. Shang, L. Ilies, E. Nakamura, *Chem. Rev.* **2017**, *117*, 9086–9139.
- [9] T. Gensch, M. J. James, T. Dalton, F. Glorius, *Angew. Chem. Int. Ed.* **2018**, *57*, 2296–2306; *Angew. Chem.* **2018**, *130*, 2318–2328.
- [10] Y. Park, Y. Kim, S. Chang, *Chem. Rev.* **2017**, *117*, 9247–9301.
- [11] T. Gensch, M. N. Hopkinson, F. Glorius, J. Wencel-Delord, *Chem. Soc. Rev.* **2016**, *45*, 2900–2936.
- [12] L. Ackermann, *Chem. Rev.* **2011**, *111*, 1315–1345.
- [13] J. B. Williamson, S. E. Lewis, R. R. Johnson, I. M. Manning, F. A. Leibfarth, *Angew. Chem. Int. Ed.* **2019**, *58*, 8654–8668; *Angew. Chem.* **2019**, *131*, 8746–8761.
- [14] Y. Segawa, T. Maekawa, K. Itami, *Angew. Chem. Int. Ed.* **2015**, *54*, 66–81; *Angew. Chem.* **2015**, *127*, 68–83.
- [15] J. Wencel-Delord, F. Glorius, *Nat. Chem.* **2013**, *5*, 369–375.
- [16] R. R. Karimov, J. F. Hartwig, *Angew. Chem. Int. Ed.* **2018**, *57*, 4234–4241; *Angew. Chem.* **2018**, *130*, 4309–4317.
- [17] W. R. Gutekunst, P. S. Baran, *Chem. Soc. Rev.* **2011**, *40*, 1976.
- [18] T. Cernak, K. D. Dykstra, S. Tyagarajan, P. Vachal, S. W. Kraska, *Chem. Soc. Rev.* **2016**, *45*, 546–576.
- [19] D. A. Colby, R. G. Bergman, J. A. Ellman, *Chem. Rev.* **2010**, *110*, 624–655.
- [20] G. Rouquet, N. Chatani, *Angew. Chem. Int. Ed.* **2013**, *52*, 11726–11743; *Angew. Chem.* **2013**, *125*, 11942–11959.
- [21] F. Zhang, D. R. Spring, *Chem. Soc. Rev.* **2014**, *43*, 6906–6919.
- [22] L. Guillemard, J. Wencel-Delord, *Beilstein J. Org. Chem.* **2020**, *16*, 1754–1804.
- [23] Y. Tang, Y. Li, F. Tao, *Chem. Soc. Rev.* **2022**, *51*, 376–423.
- [24] Z. Yang, M. L. Stivanin, I. D. Jurberg, R. M. Koenigs, *Chem. Soc. Rev.* **2020**, *49*, 6833–6847.
- [25] C. Empel, S. Jana, R. M. Koenigs, *Molecules* **2020**, *25*, 880.
- [26] D. Zhu, L. Chen, H. Fan, Q. Yao, S. Zhu, *Chem. Soc. Rev.* **2020**, *49*, 908–950.
- [27] H. M. L. Davies, J. R. Manning, *Nature* **2008**, *451*, 417–424.
- [28] F. Collet, C. Lescot, P. Dauban, *Chem. Soc. Rev.* **2011**, *40*, 1926.
- [29] G. Dequierez, V. Pons, P. Dauban, *Angew. Chem. Int. Ed.* **2012**, *51*, 7384–7395; *Angew. Chem.* **2012**, *124*, 7498–7510.
- [30] O. Baslé, *Curr. Opin. Green Sustainable Chem.* **2021**, *32*, 100539.
- [31] R. Kancherla, K. Muralirajan, A. Sagadevan, M. Rueping, *Trends Chem.* **2019**, *1*, 510–523.
- [32] P. Gandeepan, T. Müller, D. Zell, G. Cera, S. Warratz, L. Ackermann, *Chem. Rev.* **2019**, *119*, 2192–2452.
- [33] A. Wiebe, T. Gieshoff, S. Möhle, E. Rodrigo, M. Zirbes, S. R. Waldvogel, *Angew. Chem. Int. Ed.* **2018**, *57*, 5594–5619; *Angew. Chem.* **2018**, *130*, 5694–5721.
- [34] M. Yan, Y. Kawamata, P. S. Baran, *Chem. Rev.* **2017**, *117*, 13230–13319.
- [35] N. Saueremann, T. H. Meyer, Y. Qiu, L. Ackermann, *ACS Catal.* **2018**, *8*, 7086–7103.
- [36] S. Tang, Y. Liu, A. Lei, *Chem* **2018**, *4*, 27–45.
- [37] J. Yoshida, A. Shimizu, R. Hayashi, *Chem. Rev.* **2018**, *118*, 4702–4730.
- [38] M. Parasram, V. Gevorgyan, *Chem. Soc. Rev.* **2017**, *46*, 6227–6240.
- [39] K. P. S. Cheung, S. Sarkar, V. Gevorgyan, *Chem. Rev.* **2022**, *122*, 1543–1625.
- [40] P. Chuentragool, D. Kurandina, V. Gevorgyan, *Angew. Chem. Int. Ed.* **2019**, *58*, 11586–11598; *Angew. Chem.* **2019**, *131*, 11710–11722.
- [41] J. Thongpaen, R. Manguin, V. Dorcet, T. Vives, C. Duhayon, M. Mauduit, O. Baslé, *Angew. Chem. Int. Ed.* **2019**, *58*, 15244–15248; *Angew. Chem.* **2019**, *131*, 15388–15392.
- [42] L. Yang, K. Semba, Y. Nakao, *Angew. Chem. Int. Ed.* **2017**, *56*, 4853–4857; *Angew. Chem.* **2017**, *129*, 4931–4935.
- [43] J. Tanaka, Y. Nagashima, A. J. Araujo Dias, K. Tanaka, *J. Am. Chem. Soc.* **2021**, *143*, 11325–11331.
- [44] P. Gandeepan, J. Koeller, K. Korvorapun, J. Mohr, L. Ackermann, *Angew. Chem. Int. Ed.* **2019**, *58*, 9820–9825; *Angew. Chem.* **2019**, *131*, 9925–9930.
- [45] A. Sagadevan, M. F. Greaney, *Angew. Chem. Int. Ed.* **2019**, *58*, 9826–9830; *Angew. Chem.* **2019**, *131*, 9931–9935.
- [46] N. Hofmann, L. Ackermann, *J. Am. Chem. Soc.* **2013**, *135*, 5877–5884.
- [47] L. Ackermann, P. Novák, *Org. Lett.* **2009**, *11*, 4966–4969.
- [48] J. Struwe, K. Korvorapun, A. Zangarelli, L. Ackermann, *Chem. Eur. J.* **2021**, *27*, 16237–16241.
- [49] A. Sagadevan, A. Charitou, F. Wang, M. Ivanova, M. Vuagnat, M. F. Greaney, *Chem. Sci.* **2020**, *11*, 4439–4443.
- [50] K. Korvorapun, J. Struwe, R. Kuniyil, A. Zangarelli, A. Casnati, M. Waeterschoot, L. Ackermann, *Angew. Chem. Int. Ed.* **2020**, *59*, 18103–18109; *Angew. Chem.* **2020**, *132*, 18259–18265.
- [51] R. Boyaala, R. Touzani, T. Roisnel, V. Dorcet, E. Caytan, D. Jacquemin, J. Boixel, V. Guerschais, H. Doucet, J.-F. Soulé, *ACS Catal.* **2019**, *9*, 1320–1328.
- [52] J. Hubrich, T. Himmler, L. Rodefeld, L. Ackermann, *ACS Catal.* **2015**, *5*, 4089–4093.
- [53] W. Li, P. B. Arockiam, C. Fischmeister, C. Bruneau, P. H. Dixneuf, *Green Chem.* **2011**, *13*, 2315.
- [54] S. Jana, C. Pei, S. B. Bahukhandi, R. M. Koenigs, *Chem Catal.* **2021**, *13*, 467–479.
- [55] G. F. Manbeck, E. Fujita, K. J. Brewer, *J. Am. Chem. Soc.* **2017**, *139*, 7843–7854.
- [56] J. Kim, D. Kim, S. Chang, *J. Am. Chem. Soc.* **2020**, *142*, 19052–19057.
- [57] K. Shin, Y. Park, M.-H. Baik, S. Chang, *Nat. Chem.* **2018**, *10*, 218–224.

Manuscript received: January 31, 2022

Accepted manuscript online: March 28, 2022

Version of record online: June 29, 2022